

Jaroslav Hrdina; Radomil Matoušek; Aleš Návrát; Petr Vašík
Nilpotent approximation of a trident snake robot controlling distribution

Kybernetika, Vol. 53 (2017), No. 6, 1118–1130

Persistent URL: <http://dml.cz/dmlcz/147088>

Terms of use:

© Institute of Information Theory and Automation AS CR, 2017

Institute of Mathematics of the Czech Academy of Sciences provides access to digitized documents strictly for personal use. Each copy of any part of this document must contain these *Terms of use*.



This document has been digitized, optimized for electronic delivery and stamped with digital signature within the project *DML-CZ: The Czech Digital Mathematics Library* <http://dml.cz>

NILPOTENT APPROXIMATION OF A TRIDENT SNAKE ROBOT CONTROLLING DISTRIBUTION

JAROSLAV HRDINA, RADOMIL MATOUŠEK, ALEŠ NÁVRAT AND PETR VAŠÍK

We construct a privileged system of coordinates with respect to the controlling distribution of a trident snake robot and, furthermore, we construct a nilpotent approximation with respect to the given filtration. Note that all constructions are local in the neighbourhood of a particular point. We compare the motions corresponding to the Lie bracket of the original controlling vector fields and their nilpotent approximation.

Keywords: robotic snake, local control, nilpotent approximation

Classification: 93B27

1. INTRODUCTION

Within this paper, we consider a trident snake robot moving on a planar surface. More precisely, it is a model when to each vertex of an equilateral triangle a leg of length 1 is attached that is endowed with a pair of passive wheels at its end. The joints of the legs to the triangle platform are motorised and thus the possible motion directions are determined uniquely. Local controllability of such mechanism is known, see [7]. Furthermore, some generalized algorithms for motion control of a nonholonomic systems have been elaborated, see e. g. [10, 11] or [4], for introduction into the topic see [13] or [20]. If the generalized coordinates are considered, the nonholonomic forward kinematic equations can be understood as a Pfaff system and its solution as a submanifold in the configuration space on which the pullback of the defining differential forms vanishes. Rachevsky–Chow Theorem implies that the appropriate nonholonomic system is locally controllable if the corresponding distribution is maximally nonintegrable in the sense that it is not integrable and the Lie algebra generated by taking Lie brackets of the vectors fields from the controlling distribution has to be of the same dimension as the configuration space. The spanned Lie algebra is then naturally endowed with a filtration which shows the way to realize the motions by means of the vector field brackets [15, 19]. In our case, the system is locally controllable and the filtration is $(3, 6)$. Note that a motion planning of nonholonomic mechanisms is an actual topic, see e. g. [14] for one possible approach.

In order to simplify the trident snake robot control, in Section 5 we construct a privileged system of coordinates with respect to the distribution given by local nonholonomic

conditions and, furthermore, in Section 6 we construct a nilpotent approximation of the transformed distribution with respect to the given filtration. Note that all constructions are local in the neighbourhood of 0.

Finally, we compare the motions generated by the Lie brackets of the original controlling vector fields and their nilpotent approximation. The accuracy is demonstrated by simulations in MATLAB.

2. PRELIMINARIES

We recall the following concepts of functions or vector fields orders and distribution weights, see [12]. Let us denote by X_1, \dots, X_m smooth vector fields on a manifold M and by $C^\infty(p)$ the set of germs of smooth functions at $p \in M$. For $f \in C^\infty(p)$ we say that the Lie derivatives $X_i f, X_i X_j f, \dots$ are nonholonomic derivatives of f of order $1, 2, \dots$. The nonholonomic derivative of order 0 of f at p is $f(p)$.

Definition 2.1. Let $f \in C^\infty(p)$. Then the nonholonomic order of f at p , denoted by $\text{ord}_p(f)$, is the biggest integer k such that all nonholonomic derivatives of f of order smaller than k vanish at p .

Note that in case $M = \mathbb{R}^n$, $m = n$ and $X_i = \partial_{x_i}$, for a smooth function f , $\text{ord}_0(f)$ is the smallest degree of monomials having nonzero coefficient in the Taylor series. In the language of nonholonomic derivatives, the order of a smooth function is given by the formula, [12]:

$$\text{ord}_p(f) = \min \left\{ s \in \mathbb{N} : \exists i_1, \dots, i_s \in \{1, \dots, m\} \text{ s.t. } (X_{i_1} \cdots X_{i_s} f)(p) \neq 0 \right\},$$

where the convention reads that $\min \emptyset = \infty$.

If we denote by $\text{VF}(p)$ the set of germs of smooth vector fields at $p \in M$, the notion of nonholonomic order extends to the vector fields as follows:

Definition 2.2. Let $X \in \text{VF}(p)$. The nonholonomic order of X at p , denoted by $\text{ord}_p(X)$, is a real number defined by:

$$\text{ord}_p(X) = \sup \left\{ \sigma \in \mathbb{R} : \text{ord}_p(Xf) \geq \sigma + \text{ord}_p(f), \forall f \in C^\infty(p) \right\}.$$

Note that $\text{ord}_p(X) \in \mathbb{Z}$. Moreover, the null vector field $X \equiv 0$ has infinite order, $\text{ord}_p(0) = \infty$. Furthermore, X_1, \dots, X_m are of order ≥ -1 , $[X_i, X_j]$ of order ≥ -2 , etc.

Using the notion of a vector field order one can define

Definition 2.3. A family of m vector fields $(\hat{X}_1, \dots, \hat{X}_m)$ defined near p is called a first order approximation of (X_1, \dots, X_m) at p if the vector fields $X_i - \hat{X}_i, i = 1, \dots, m$ are of order ≥ 0 at p .

Finally, to define the weights of distributions we use the same notation as in [12]. Let us by Δ^1 denote the distribution

$$\Delta^1 = \text{span}\{X_1, \dots, X_m\}$$

and for $s \geq 1$ define

$$\Delta^{s+1} = \Delta^s + [\Delta^1, \Delta^s],$$

where $[\Delta^1, \Delta^s] = \text{span}\{[X, Y] : X \in \Delta^1, Y \in \Delta^s\}$. Note that this directly leads to the fact that every $X \in \Delta^s$ is of order $\geq -s$. Now let us consider the sequence

$$\Delta^1(p) \subset \Delta^2(p) \subset \dots \subset \Delta^{r-1} \subsetneq \Delta^r(p) = T_pM,$$

where $r = r(p)$ is called the degree of nonholonomy at p . Set $n_i(p) = \dim \Delta^i(p)$. Then we can define the weights at p , $w_i = w_i(p), i = 1, \dots, n = n_{r(p)}$ by setting $w_j = s$ if $n_{s-1}(p) < j \leq n_s(p)$, where $n_0 = 0$. In other words, we have

$$w_1 = \dots = w_{n_1} = 1, w_{n_1+1} = \dots = w_{n_2} = 2, \dots, w_{n_{r-1}+1} = \dots = w_{n_r} = r.$$

The weights at p form an increasing sequence $w_1(p) \leq \dots \leq w_n(p)$.

3. TRIDENT SNAKE ROBOT

The mechanism of the trident snake robot was introduced in [7]. It consists of a body in the shape of an equilateral triangle with circumscribed circle of radius r and three rigid links (also called legs) of constant length l connected to the vertices of the triangular body by three motorised joints. In this paper, we consider $r = 1$ and $l = 1$ although an arbitrary number of links can be attached. For an efficient tool for more extensive robots in the form of conformal geometric algebra we refer to [5, 6] or [16]. To each free link end, a pair of passive wheels is attached to provide an important snake-like property that the ground friction in the direction perpendicular to the link is considerably higher than the friction of a simple forward move. In particular, this prevents slipping sideways. To describe the actual position of a trident snake robot we need the set of 6 generalized coordinates

$$q = (x, y, \theta, \phi_1, \phi_2, \phi_3) =: (x_1, x_2, x_3, x_4, x_5, x_6)$$

as shown in Figure 1. Hence the configuration space is (a subspace of) $\mathbb{R}^2 \times S^1 \times (S^1)^3$. Note that a fixed coordinate system (x, y) is attached. For further studies of more complicated trident snake robots see e.g. [8], for the description of the dynamics see [18].

4. LOCAL CONTROLLABILITY AND COORDINATE SYSTEMS

Local controllability of such robot is given by the appropriate Pfaff system of ODEs. To find more details about the connection between dynamical system and geometric control theory we refer to e.g. [2]. According to [7], the appropriate nonholonomic constraints give a control system $\dot{q} = G\mu$, where the control matrix G is a 6×3 matrix spanned by vector fields g_1, g_2, g_3 , where

$$\begin{aligned} g_1 &= \cos \theta \partial_x + \sin \theta \partial_y + \sin \phi_1 \partial_{\phi_1} + \sin(\phi_2 + \frac{2\pi}{3}) \partial_{\phi_2} + \sin(\phi_3 + \frac{4\pi}{3}) \partial_{\phi_3}, \\ g_2 &= -\sin \theta \partial_x + \cos \theta \partial_y - \cos \phi_1 \partial_{\phi_1} - \cos(\phi_2 + \frac{2\pi}{3}) \partial_{\phi_2} - \cos(\phi_3 + \frac{4\pi}{3}) \partial_{\phi_3}, \\ g_3 &= \partial_\theta - (1 + \cos \phi_1) \partial_{\phi_1} - (1 + \cos \phi_2) \partial_{\phi_2} - (1 + \cos \phi_3) \partial_{\phi_3}. \end{aligned}$$

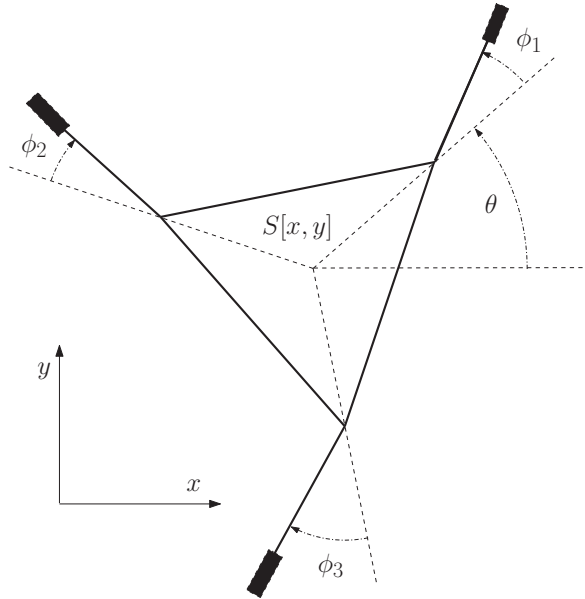


Fig. 1: Trident snake robot model.

Note that the parametrizations can vary by setting the angles within the triangular platform either $\frac{2\pi}{3}$ and $\frac{4\pi}{3}$ or $\frac{2\pi}{3}$ and $-\frac{2\pi}{3}$, etc. It is easy to check that in regular points these vector fields define a (bracket generating) distribution with growth vector (3, 6). It means that in each regular point the vector fields g_1, g_2, g_3 together with their Lie brackets span the whole tangent space. Consequently, the system is controllable by Chow–Rashevsky theorem.

Let us decompose the control system in such way that the spatial coordinates $w := (x, y, \theta) = (x_1, x_2, x_3)$ are parametrized by the angles $\phi := (\phi_1, \phi_2, \phi_3) = (x_4, x_5, x_6)$, and, furthermore, the invariant parameter θ is excluded, i. e. it is of the form

$$A(\phi)R_\theta^T \dot{w} = \dot{\phi}, \tag{1}$$

where

$$R_\theta^T = \begin{pmatrix} \cos \theta & \sin \theta & 0 \\ -\sin \theta & \cos \theta & 0 \\ 0 & 0 & 1 \end{pmatrix}$$

is the matrix of rotation by the angle θ , see [9]. If the spatial coordinate transformation

$$v = (A(\phi))^{-1} \dot{\phi} \tag{2}$$

is considered, we modify the system (1) and obtain

$$\dot{w} = R_\theta (A(\phi))^{-1} \dot{\phi} = R_\theta v.$$

Consequently, the Lie algebra generating vector fields g_1, g_2, g_3 are transformed as follows:

$$\begin{aligned}
 g_1 &= \partial_{x_1} + \sin(x_4 - \frac{2\pi}{3})\partial_{x_4} + \sin(x_5)\partial_{x_5} + \sin(x_6 + \frac{2\pi}{3})\partial_{x_6}, \\
 g_2 &= \partial_{x_2} - \cos(x_4 - \frac{2\pi}{3})\partial_{x_4} - \cos(x_5)\partial_{x_5} - \cos(x_6 + \frac{2\pi}{3})\partial_{x_6}, \\
 g_3 &= \partial_{x_3} - (1 + \cos(x_4))\partial_{x_4} - (1 + \cos(x_5))\partial_{x_5} - (1 + \cos(x_6))\partial_{x_6}.
 \end{aligned}
 \tag{3}$$

We shall use this form for the sake of simplicity. Furthermore, to demonstrate the effects of the Lie algebra motions, we calculate the vector fields given by the Lie brackets of g_1, g_2, g_3 evaluated at 0 and denote them by $g_4 = [g_1, g_2], g_5 = [g_2, g_3]$ and $g_6 = [g_1, g_3]$. Their coordinate form with respect to the system (2) is the following:

$$\begin{aligned}
 g_4 &= \partial_{x_4} + \partial_{x_5} + \partial_{x_6}, \\
 g_5 &= \sqrt{3}\partial_{x_5} - \sqrt{3}\partial_{x_6}, \\
 g_6 &= 2\partial_{x_4} - \partial_{x_5} - \partial_{x_6}.
 \end{aligned}
 \tag{4}$$

Following [7] we demonstrate the motions which approximate the Lie brackets motions. By the Lie bracket motions we mean motions generated by g_4, g_5, g_6 which are not in the distribution and thus not allowed. Further details of the Lie bracket exact realizations are described in Section 7 and can be found in [7]. The following figures show the trajectories of the root centre point, vertices and wheels when a particular Lie bracket motion is realized. Note that the trajectories on Figure 2 read that the

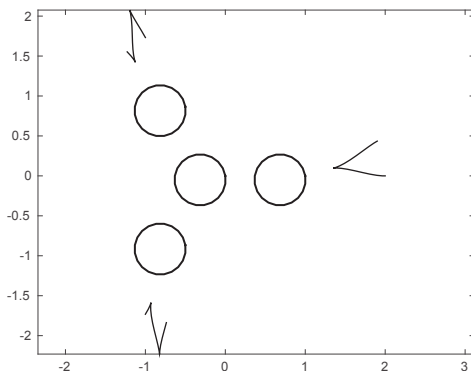


Fig. 2: Realization of g_4 motion.

root stays put and the angles represented by the coordinates x_4, x_5, x_6 change, which is obvious from approximately equal dislocation of the wheel points at the end of the motion. Considering the vector field g_4 at 0 one finds that the angles should change proportionally to 1:1:1. Similarly, Figure 3 demonstrates the Lie bracket g_5 motion and clearly the trajectories represent the effect that the root moves along the x -axis and the angles change proportionally to 1:0:-1. Finally, Figure 4 shows g_6 realization which reads that the root moves along the y -axis and the angles change proportionally to -2:1:1.

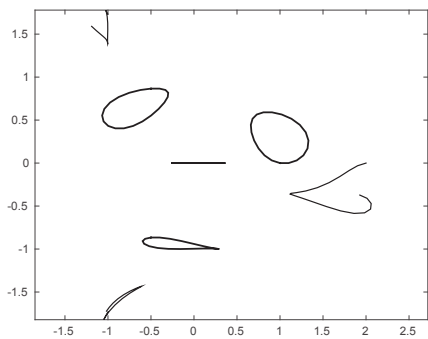


Fig. 3: Realization of g_5 motion.

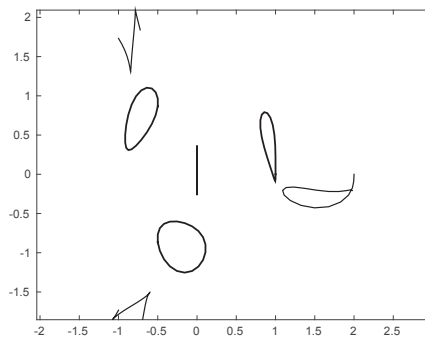


Fig. 4: Realization of g_6 motion.

5. PRIVILEGED COORDINATES

A general definition of privileged coordinates is the following, [12], taking into account the notation from Section 2.

Definition 5.1. A system of privileged coordinates at p is a system of local coordinates (y_1, \dots, y_n) such that $\text{ord}_p(y_j) = w_j$ for $j = 1, \dots, n$.

In our case the configuration space of the trident snake robot is a 6–dimensional manifold M with the coordinate functions denoted by

$$(x, y, \theta, \phi_1, \phi_2, \phi_3) =: (x_1, x_2, x_3, x_4, x_5, x_6).$$

Let the basis of vector space T_pM be denoted by

$$(\partial_{x_1}, \partial_{x_2}, \partial_{x_3}, \partial_{x_4}, \partial_{x_5}, \partial_{x_6}),$$

and let us consider three vector fields g_1, g_2, g_3 in the form (3) which determine a distribution in TM , and we add their Lie brackets g_4, g_5, g_6 , see (4). Note that this establishes a filtration of type (3, 6) on TM . The first question is what is the exact form of a coordinate transformation $x := (x_1, x_2, x_3, x_4, x_5, x_6) \rightsquigarrow (y_1, y_2, y_3, y_4, y_5, y_6) =: y$ such that the condition

$$\frac{\partial}{\partial y_i} \Big|_p = g_i \Big|_p, \quad i = 1, \dots, 6 \tag{5}$$

holds in $p \in M$. Let us denote by $[g_k^i]_y$ the i th coordinate of vector g_k in the coordinate system y and by e^i a 6–dimensional vector with coordinates $e_j^i = 0$ for $i \neq j$ and $e_j^i = 1$ for $i = j, i, j \in \{1, \dots, 6\}$. Then e.g. $[g_1^1]_x = 1, [g_1^2]_x = 0, [g_1^3]_x = 0, [g_1^4]_x = \sin(x_3 + x_6)$ etc. and the condition (5) reads $[g_i]_y = e^i$. Employing the Einstein summation convention, i.e. summing over j ranging from 1 to 6, the transformation law for vector fields under the coordinate change $x \rightsquigarrow y$ reads

$$[g_k^i]_y = \frac{\partial y_i}{\partial x_j} [g_k^j]_x.$$

Particularly, in the vector form we have

$$e^i = [g_i]_y = \begin{pmatrix} \frac{\partial y_1}{\partial x_j} \left[g_i^j \right]_x \\ \frac{\partial y_2}{\partial x_j} \left[g_i^j \right]_x \\ \vdots \\ \frac{\partial y_6}{\partial x_j} \left[g_i^j \right]_x \end{pmatrix}.$$

Evaluating all functions at an arbitrary point p , for sake of simplicity we choose the point $p = (0, 0, 0, 0, 0, 0)$, we get a system of 36 linear PDEs with respect to $\frac{\partial y_i}{\partial x_j}$ with constant coefficients. We split the system into 6 groups, each containing 6 equations for a particular y_i , determine the inverse matrix and continue by integration. Clearly, at an arbitrary $p \in M$ the desired transformation $x \rightsquigarrow y$ will be linear, in our case it will be given by

$$\begin{pmatrix} y_1 \\ y_2 \\ y_3 \\ y_4 \\ y_5 \\ y_6 \end{pmatrix} = \begin{pmatrix} 1 & 0 & 0 & 0 & 0 & 0 \\ 0 & 1 & 0 & 0 & 0 & 0 \\ 0 & 0 & 1 & 0 & 0 & 0 \\ \frac{\sqrt{3}}{2} & \frac{1}{2} & -2 & 1 & -1 & \sqrt{3} \\ 0 & -1 & -2 & 1 & 2 & 0 \\ -\frac{\sqrt{3}}{2} & \frac{1}{2} & -2 & 1 & -1 & -\sqrt{3} \end{pmatrix} \begin{pmatrix} x_1 \\ x_2 \\ x_3 \\ x_4 \\ x_5 \\ x_6 \end{pmatrix}. \tag{6}$$

The coordinates $y = (y_1, y_2, y_3, y_4, y_5, y_6)$ are clearly the privileged ones.

6. NILPOTENT APPROXIMATION

We proceed according to Bellaïche’s algorithm. To find further details about nilpotent approximations in full generality we refer to [3, 21] while another type of approximation of a nonholonomic system can be found in [1]. To find a computation of a nilpotent approximation of a robotic snake model we refer to [17]. Note that in the sequel we use the first two steps only due to the fact that in our filtration (3,6) of $T_p M$ the weights at p are 1 and 2 and thus no further modification of the coordinate system is needed, see [12] for a detailed explanation and proof. Let us consider the vector fields g_1, g_2, g_3 from Section 5 expressed in the privileged coordinate system $y = (y_1, y_2, y_3, y_4, y_5, y_6)$.

Vector fields g_i are of order ≥ -1 and thus generally their Taylor expansion is of the form:

$$g_i(y) \sim \sum_{\alpha, j} a_{\alpha, j} y^\alpha \partial_{y_j},$$

where $\alpha = (\alpha_1, \dots, \alpha_n)$ is a multiindex. Furthermore, if we define a weighted degree of the monomial $y^\alpha = y_1^{\alpha_1} \dots y_n^{\alpha_n}$ to be $w(\alpha) = w_1 \alpha_1 + \dots + w_n \alpha_n$, then $w(\alpha) \geq w_j - 1$ if $a_{\alpha, j} \neq 0$. Recall that $w_j = \text{ord}_p(y_j)$ from Definition 5.1 and in our particular case the coordinate weights are $(1, 1, 1, 2, 2, 2)$. Grouping together the monomial vector fields of the same weighted degree we express $g_i, i = 1, 2, 3$ as a series

$$g_i = g_i^{(-1)} + g_i^{(0)} + g_i^{(1)} + \dots,$$

where $g_i^{(s)}$ is a homogeneous vector field of degree s . Note that this means that the $\partial_{y_1}, \partial_{y_2}$ and ∂_{y_3} coordinate functions of $g_1^{(-1)}, g_2^{(-1)}$ and $g_3^{(-1)}$ are formed by constants and the $\partial_{y_4}, \partial_{y_5}$ and ∂_{y_6} coordinate functions are linear polynomials in y_1, y_2, y_3 . Then the following proposition holds, [12]:

Proposition 6.1. Set $\hat{g}_i = g_i^{(-1)}, i = 1, 2, 3$. The family of vector fields $\{\hat{g}_1, \hat{g}_2, \hat{g}_3\}$ is a first order approximation of $\{g_1, g_2, g_3\}$ at 0 and generates a nilpotent Lie algebra of step $r = 1$, i. e. all brackets of length greater than 1 are zero.

Proof. In our case in coordinate form given by (6), we obtain the following vector fields:

$$\begin{aligned} \hat{g}_1 &= \partial_{y_1} - \frac{y_2}{2}\partial_{y_4} + \left(-\frac{y_2}{2} - y_3\right)\partial_{y_5} - \frac{y_1}{2}\partial_{y_6}, \\ \hat{g}_2 &= \partial_{y_2} + \frac{y_1}{2}\partial_{y_4} - \frac{y_1}{2}\partial_{y_5} + \left(\frac{y_2}{2} - y_3\right)\partial_{y_6}, \\ \hat{g}_3 &= \partial_{y_3}. \end{aligned}$$

Note that due to linearity of the three latter coordinates of $\{\hat{g}_1, \hat{g}_2, \hat{g}_3\}$, the coordinates of their Lie brackets $\{\hat{g}_4, \hat{g}_5, \hat{g}_6\}$ must be constant. Indeed, we get

$$\begin{aligned} \hat{g}_4 &= \partial_{y_4} \\ \hat{g}_5 &= \partial_{y_5} \\ \hat{g}_6 &= \partial_{y_6} \end{aligned}$$

and the nilpotency is obvious. It is also easy to see that the value in 0 coincides with the columns of matrix in (6) and thus the family $\{\hat{g}_1, \hat{g}_2, \hat{g}_3\}$ is the nilpotent approximation of $\{g_1, g_2, g_3\}$ at 0. □

7. LIE BRACKET MOTION EFFECTS

In the following, we compare the effect of the Lie bracket motions in the original coordinate system and in the nilpotent approximation. To do so we follow the structure of [7], yet to compare the vector fields in the same coordinate system, the inverse transformation must be applied first and the evaluation of the vector fields effects must be done consequently. Note that the vector fields $\{\hat{g}_1, \hat{g}_2, \hat{g}_3, \hat{g}_4, \hat{g}_5, \hat{g}_6\}$ in $(x_1, x_2, x_3, x_4, x_5, x_6)$ coordinates are of the form

$$\begin{aligned} \hat{g}_1 &= \partial_{x_1} - (x_2 + x_3)\partial_{x_4} - \left(\frac{\sqrt{3}x_1}{4} + \frac{x_2}{4} - \frac{x_3}{2} - \frac{\sqrt{3}}{2}\right)\partial_{x_5} + \\ &\quad + \left(\frac{\sqrt{3}x_1}{2} - \frac{x_2}{4} + \frac{x_3}{2} - \frac{\sqrt{3}}{2}\right)\partial_{x_6}, \\ \hat{g}_2 &= \partial_{x_2} - \partial_{x_4} + \left(\frac{3x_1}{4} + \frac{\sqrt{3}x_2}{4} - \frac{\sqrt{3}x_3}{2} + \frac{1}{2}\right)\partial_{x_5} + \left(\frac{3x_1}{4} - \frac{\sqrt{3}x_2}{4} + \frac{\sqrt{3}x_3}{2} + \frac{1}{2}\right)\partial_{x_6}, \\ \hat{g}_3 &= \partial_{x_3} - 2\partial_{x_4} - 2\partial_{x_5} - 2\partial_{x_6} \\ \hat{g}_4 &= \partial_{x_4} + \partial_{x_5} + \partial_{x_6}, \\ \hat{g}_5 &= -\frac{\sqrt{3}}{2}\partial_{x_5} + \frac{\sqrt{3}}{2}\partial_{x_6}, \\ \hat{g}_6 &= -\partial_{x_3} + \frac{1}{2}\partial_{x_5} + \frac{1}{2}\partial_{x_6}. \end{aligned}$$

Note that the Lie bracket motions at 0 correspond exactly to the original ones. Anyway, to perform the Lie bracket motions we apply a periodic input, i. e. for the vector fields $\hat{g}_4 = [\hat{g}_1, \hat{g}_2]$, $\hat{g}_5 = [\hat{g}_1, \hat{g}_3]$, $\hat{g}_6 = [\hat{g}_2, \hat{g}_3]$, respectively, the input

$$v_1(t) = (-A\omega \sin \omega t, A\omega \cos \omega t, 0) \quad (7)$$

$$v_2(t) = (0, -A\omega \sin \omega t, A\omega \cos \omega t) \quad (8)$$

$$v_3(t) = (-A\omega \sin \omega t, 0, A\omega \cos \omega t) \quad (9)$$

is applied, because, according to [7], the Lie bracket of a pair of vector fields corresponds to the direction of a displacement in the state space as a result of a periodic input with sufficiently small amplitude A , i. e. the bracket motions are generated by periodic combination of the vector controlling fields. In Figure 5, there is a comparison of the g_4 motion realized by the periodic input in x_1, \dots, x_6 coordinates (dotted line) and in nilpotent approximation for $A = 0.35$ and $\omega = 2\pi/100$.

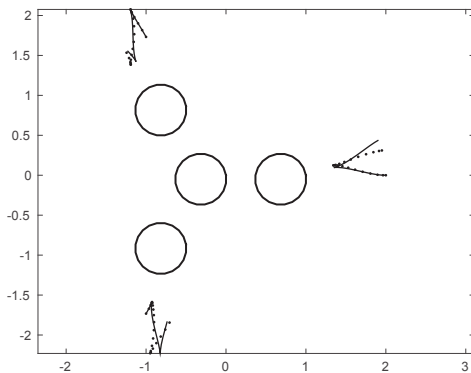


Fig. 5: Comparison of g_4 motions.

Figure 6 and 7 show the comparison of g_5 and g_6 motions, respectively. Note that the lines represent the trajectories of the appropriate wheel and thus the accuracy of the motion in real space is pictured.

Figures 8, 9 and 10 display the comparison of the shape angles x_1, x_2, x_3 during g_4, g_5 and g_6 motions, respectively. Figures 11, 12 and 13 show the maximal difference between the shape angles of the robot controlled by the original vector fields and their nilpotent approximation during g_4, g_5 and g_6 motions, respectively.

The following table shows the dependence of the maximal deviation of x_1, x_2, x_3 on the amplitude A during g_4 motions.

A	0.15	0.25	0.35	0.45	0.55
x_4	0.01	0.06	0.18	0.43	0.86
x_5	0.01	0.06	0.18	0.41	0.72
x_6	0.01	0.04	0.10	0.21	0.36

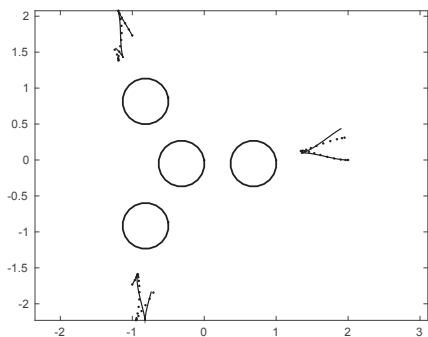


Fig. 6: Comparison of g_5 motions.

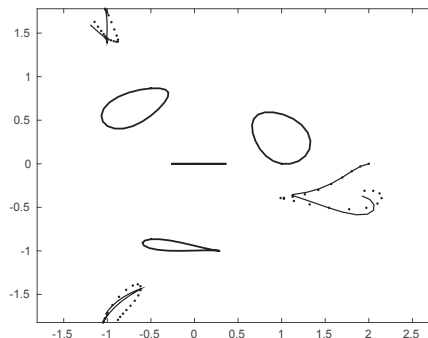


Fig. 7: Comparison of g_6 motions.

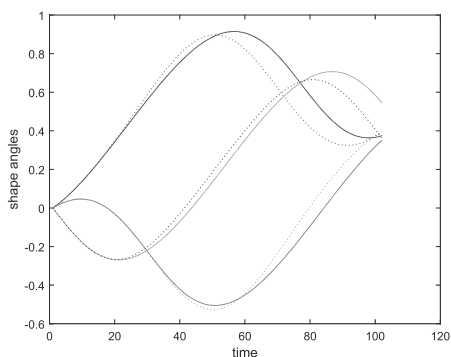


Fig. 8: Comparison of x_1, x_2, x_3 during g_4 motion.

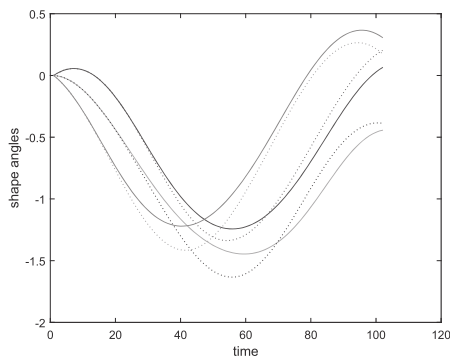


Fig. 9: Comparison of x_1, x_2, x_3 during g_5 motion.

8. CONCLUSIONS

We presented a calculation of a nilpotent approximation of the family of vector fields corresponding to the controlling distribution of a trident snake robot. Such an approximation is valuable not only for the calculational complexity reasons but also from the theoretical point of view as the nilpotency simplifies the model for further theoretical considerations significantly. We showed that even from the practical point of view this approximation is good as the deviation from the exact model control is minimal. More precisely, we checked that at 0 the Lie brackets of the original controlling vector fields and of the approximated ones coincide and, furthermore, if their realization by the periodic input is considered, the deviations depicted in Figures 5, 6, 7 are minimal. Finally let us claim that the error in control leads to the violation of the nonholonomic conditions and thus the wheels slip a bit, yet the benefits of the nilpotent approximation prevail.

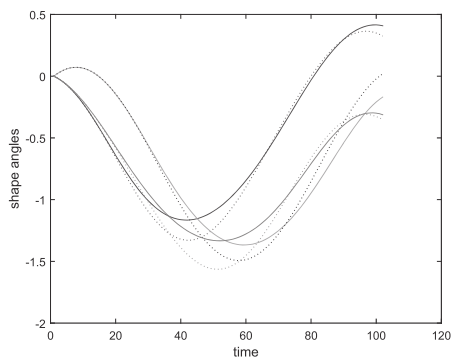


Fig. 10: Comparison of x_1, x_2, x_3 during g_6 motion.

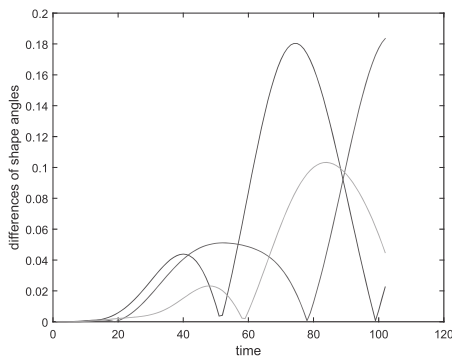


Fig. 11: Deviation of x_1, x_2, x_3 during g_4 motion.

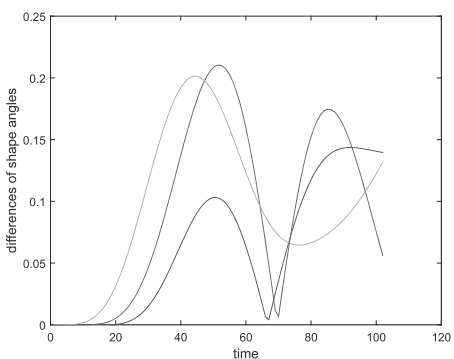


Fig. 12: Deviation of x_1, x_2, x_3 during g_5 motion.

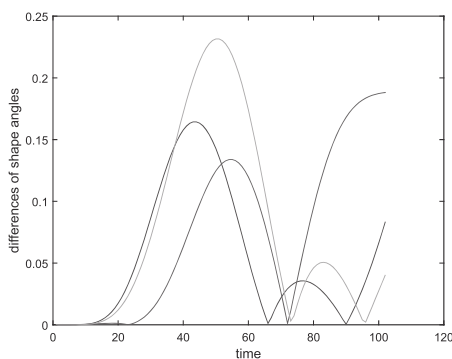


Fig. 13: Deviation of x_1, x_2, x_3 during g_6 motion.

ACKNOWLEDGEMENT

The research has been supported by the Project LO1202 (funded by the MEYS under the National Sustainability Programme I).

(Received January 23, 2017)

REFERENCES

[1] Ma Bao-Li: Local exponential regulation of nonholonomic systems in approximate chained form with applications to off-axle tractor-trailers. *J. Robotics 2007* (2007), 1–8. DOI:10.1155/2011/697309

- [2] Q. Cai, T. Huang, Y. L. Sachkov, and X. Yang: Geodesics in the Engel group with a sub-Lorentzian metric. *J. Dynamical Control Systems* *22* (2016), 465–483. DOI:10.1007/s10883-015-9295-2
- [3] H. Hermes: Nilpotent approximations of control systems and distributions. *Siam J. Control Optim.* *24* (1986), 731–736. DOI:10.1137/0324045
- [4] J. Hrdina: Local controllability of trident snake robot based on sub-Riemannian extremals. *Note di Matematica* *37* (2017), 93–102.
- [5] J. Hrdina, A. Návrát, P. Vašík, and R. Matoušek: Geometric Control of the Trident Snake Robot Based on CGA. *Adv. Appl. Clifford Algebr.* *27* (2017), 633–645. DOI:10.1007/s00006-016-0693-7
- [6] J. Hrdina, A. Návrát, P. Vašík, and R. Matoušek: CGA-based robotic snake control. *Adv. Appl. Clifford Algebr.* *27* (2017), 633–645. DOI:10.1007/s00006-016-0693-7
- [7] M. Ishikawa: Trident snake robot: Locomotion analysis and control. In: *Proc. IFAC NOLCOS, IFAC Nonlinear Control Systems, Stuttgart 2004*, pp. 1169–1174. DOI:10.1016/s1474-6670(17)31339-3
- [8] M. Ishikawa and T. Fukiro: Control of the double-linked trident snake robot based on the analysis of its oscillatory dynamics. In: *Proc. IEEE/RSJ IROS 2009*, pp. 1314–1319. DOI:10.1109/iros.2009.5354831
- [9] M. Ishikawa, Y. Minami, and T. Sugie: Development and control experiment of the trident snake robot. *IEEE/ASME Trans. Mechatron.* *15* (2010), 9–16. DOI:10.1109/tmech.2008.2011985
- [10] J. Jakubiak, K. Tchon, and M. Janiak: Motion planning of the trident snake robot: an endogenous configuration space approach. In: *ROMANSY 18 Robot Design, Dynamics and Control: Proc. Eighteenth CISM-IFToMM Symposium* (V. P. Castelli and W. Schiehlen, eds.), Springer, Vienna 2010, pp. 159–166. DOI:10.1007/978-3-7091-0277-0_18
- [11] E. Jarzebowska: Stabilizability and motion tracking conditions for mechanical nonholonomic control systems. *Math. Problems Engrg.* *2007* (2007), 1–20. DOI:10.1155/2007/31267
- [12] F. Jean: *Control of Nonholonomic Systems: From Sub-Riemannian Geometry to Motion Planning*. Springer International Publishing, New York 2014. DOI:10.1007/978-3-319-08690-3
- [13] P. Liljeback, K. Y. Pettersen, Ø. Stavdahl, and J. T. Gravdahl: *Snake Robots, Modelling, Mechatronics and Control*. Springer-Verlag, London 2013. DOI:10.1007/978-1-4471-2996-7
- [14] O. Meiyong, G. Shengwei, W. Xianbing, and D. Kexiu: Finite-time tracking control of multiple nonholonomic mobile robots with external disturbances. *Kybernetika* *51* (2015), 1049–1067. DOI:10.14736/kyb-2015-6-1049
- [15] R. M. Murray, L. Zexiang, and S. S. Sastry: *A Mathematical Introduction to Robotic Manipulation*. CRC Press, Boca Raton 1994.
- [16] A. Návrát and R. Matoušek: Trident snake control based on CGA. *Mendel 2015: Recent Advances in Computer Science* *378* (2015), 375–385. DOI:10.1007/978-3-319-19824-8_31
- [17] A. Návrát and P. Vašík: On geometric control models of a robotic snake. *Note di Matematica* *37* (2017), 119–129.
- [18] Z. Pietrowska and K. Tchon: Dynamics and motion planning of trident snake robot. *J. Intelligent Robotic Systems* *75* (2014), 17–28. DOI:10.1007/s10846-013-9858-y
- [19] J. M. Selig: *Geometric Fundamentals of Robotics*. Second edition. Springer, New York 2004. DOI:10.1017/s0263574706262805

- [20] A. A. Transeth, K. Y. Pettersen, and P. Liljebäck: A survey on snake robot modeling and locomotion. *Robotica* 27 (2009), 999–1015. DOI:10.1017/s0263574709005414
- [21] M. Venditelli, G. Oriolo, F. Jean, and J. P. Laumond: Nonhomogeneous nilpotent approximations for nonholonomic systems with singularities. *IEEE Trans. Automat. Control* 49 (2004), 261–266. DOI:10.1109/tac.2003.822872

*Jaroslav Hrdina, Brno University of Technology, Faculty of Mechanical Engineering, Institute of Mathematics, Technická 2896/2, 616 69 Brno. Czech Republic.
e-mail: hrdina@fme.vutbr.cz*

*Radomil Matoušek, Brno University of Technology, Faculty of Mechanical Engineering, Institute of Mathematics, Technická 2896/2, 616 69 Brno. Czech Republic.
e-mail: matousek@fme.vutbr.cz*

*Aleš Návrat, Brno University of Technology, Faculty of Mechanical Engineering, Institute of Mathematics, Technická 2896/2, 616 69 Brno. Czech Republic.
e-mail: navrat.a@fme.vutbr.cz*

*Petr Vašík, Brno University of Technology, Faculty of Mechanical Engineering, Institute of Mathematics, Technická 2896/2, 616 69 Brno. Czech Republic.
e-mail: vasik@fme.vutbr.cz*